Communication

Antenna Array Diagnosis Using a Deep Learning Approach

He Ming Yao, Min Li, Lijun Jiang, Kwan Lawrence Yeung, and Michael Ng

***Abstract*— In this communication, we propose to use a deep learning (DL) approach to detect unit failure in array antennas. Due to natural machine life cycle and/or unexpected accidents, antenna units unavoidably suffer from the risk of failure, leading to the deterioration of array performance. To realize the detection of unit failure, the far-field radiation patterns are used as the input of the deep convolutional neural network (DConvNet) for antenna array diagnosis learning. The proposed DConvNet consists of continuous functional groups of convolution, batch normalization, and activation layers, followed by a fully connected layer to realize recognition, i.e., the fault diagnosis of antenna array. Different from conventional diagnosis techniques, the main advantage of the proposed DL approach does not require intensive computations based on Green's function. The training data are collected by the electromagnetic (EM) simulation tool. Additionally, the Gaussian noise is added to the training data to imitate the interference in real application scenarios. The proposed DConvNet for array diagnosis is verified by three numerical benchmarks and demonstrates that it can diagnose antenna array in a complex environment with generality.**

***Index Terms*— Antenna arrays, convolutional neural network, deep learning (DL), fault diagnosis.**

I. Introduction

Antenna arrays are widely utilized in electromagnetic (EM) radiation scenarios, including radar detection, far-field imaging, and remote sensing [1], [2], [3], [4]. Keeping a proper and stable working state of antenna units is of great importance [1], [2], [3], [4]. However, either used in open space or packaged in enclosed devices, antennas units unavoidably suffer from the risk of failure (e.g., machine aging, sudden accidents, or atmospheric conditions, including snow, ice, and dirt) [4], [5], [6], [7]. The failure of one (or more) unit(s) could tremendously harm the system performances [5], [6], [7], such as increasing the mismatching loss, lowering the radiation efficiency, and deteriorating the radiation pattern. Thus, the detect of unit failure in array antennas have been attracting extensive attention [7].

Several techniques have been proposed for array diagnosis. The optimization methods, including genetic algorithms [8] and exhaustive search [9], were widely used to identify the locations of the faulty antenna units. However, it requires the comparison between the radiation pattern of the array under test (AUT) and that of the reference array, leading to complicated measurement and computation [8], [9]. To simplify the measurement and computation in optimization methods, the diagnostic techniques based on compressed sensing (CS) were reported in [10] and [11]. However, the required long diagnosis time in CS-based techniques [10], [11] could limit its wide applications. Hence, besides the conventional techniques, the development of fault diagnosis techniques for antenna arrays with higher efficiency and accuracy is still in great request.

Machine learning (ML) techniques have been introduced to every corner of traditional EM research [12], [13], particularly the deep learning (DL) technique [14]. Recently, there are many significant applications, such as scientific computing [15], [16], [17], [18], microwave engineering [19], [20], and field-circuit cosimulation [21], [22]. For instance, [18] proposed a DL-based method to realize EM forward process. In [16] and [17], a solver employing DL technique was described for addressing Poisson's equations, which facilitated the computation of potential distributions across both 2-D and 3-D settings. Some DL-based methods were reported to help solve problems related to finite-difference time-domain (FDTD) method [23], [24], [25]. A large number of DL methods have been proposed to solve EM inverse problems and demonstrate better performance. The learning-assisted multimodality is proposed to recover human brain dielectric images with single-frequency and multifrequency microwave measurements [52]. Plus, the physics-assisted learning methods, where domain knowledge is incorporated either in DL model [53], [54], have been successfully applied to microwave imaging and biomedical imaging. Moreover, [55] attempt to embed DL in inverse scattering problems, where a DL-based framework to solve EMIS problems and demonstrate the ability to recover high permittivity objects. The ML approaches have also been used in antenna areas, such as antenna design [26], radiation computation [27], [28], and subwavelength imaging [32]. Compared with conventional methods, the ML approach could solve some EM problems more efficiently. For the application of ML techniques to antenna diagnosis, some machine-learning-based methods have to make use of training data collected from complicated derivation and computation based on mathematical formula to do diagnosis [56], [57], [58], which suffer from complexity and increase computation cost. On the contrary, other reported works have to make use of complex measurement system, including complex near-field measurement, to collect data and do further prediction [59], which also increase extra cost and computation complexity for the diagnosis. Besides, the work about cascading two deep neural networks to realize antenna array diagnosis is also reported [60], but its structure will increase computation cost both in training and in computation.

This communication proposes to utilize the deep convolutional neural network (DConvNet) to realize the fault diagnosis in array antennas with high accuracy and efficiency. The proposed DConvNet consists of continuous functional groups of convolution, batch normalization, and activation layers, followed by a fully connected layer to realize the recognition, i.e., the fault diagnosis of antenna array. The radiation patterns in the far-field collected from EM simulation tool are utilized as the input (training data) of the DConvNet. The merits of this DL approach can be encapsulated as follows.

1) *Anti-interference*: This approach is of strong resistance to interference with high precision, despite large

Manuscript received 1 November 2020; revised 18 June 2022; accepted 19 June 2022. Date of publication 9 May 2024; date of current version 7 June 2024. This work was supported in part by Hong Kong Research Grants Council (HKRGC) General Research Fund (GRF) under Grant 17201020 and Grant 17300021; in part by HKRGC Collaborative Research Fund (CRF) under Grant C7004-21GF; in part by the Joint NSFC and Research Grants Council (RGC) under Grant N-HKU769/21; and in part by RGC of Hong Kong Special Administrative Region, China, under Grant HKU PDFS2122-7S05. *(Corresponding author: Min Li.)*

He Ming Yao is with the Department of Mathematics, The University of Hong Kong, Hong Kong, China (e-mail: yaohmhk@connect.hku.hk).

Min Li, Lijun Jiang, and Kwan Lawrence Yeung are with the Department of Electrical and Electronic Engineering, The University of Hong Kong, Hong Kong, China (e-mail: minli@hku.hk; jianglj@hku.hk; kyeung@eee.hku.hk).

Michael Ng is with the Department of Mathematics, Hong Kong Baptist University, Hong Kong, China (e-mail: michael-ng@hkbu.edu.hk).

Color versions of one or more figures in this article are available at https://doi.org/10.1109/TAP.2024.3387689.

Digital Object Identifier 10.1109/TAP.2024.3387689

0018-926X © 2024 IEEE. Personal use is permitted, but republication/redistribution requires IEEE permission.
See https://www.ieee.org/publications/rights/index.html for more information.
Authorized licensed use limited to: Missouri University of Science and Technology. Downloaded on January 16,2025 at 18:20:40 UTC from IEEE Xplore. Restrictions apply.

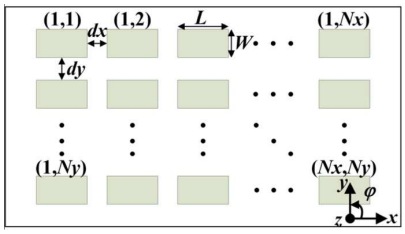

Fig. 1. Two-dimensional planar antenna array.

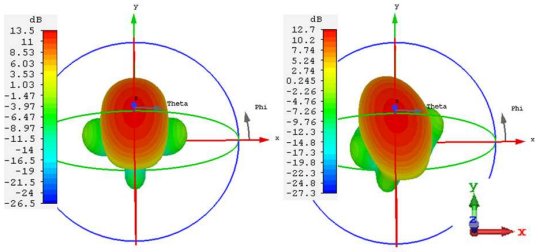

(a) (b)

Fig. 2. Three-dimensional radiation patterns of a 3 × 3 patch array. (a) Without unit failure. (b) With the failure of the first unit (1,1).

interference (noise) integrated to the radiation of antenna system.

2) *Simplicity*: During the diagnosing process, the antenna mutual coupling is automatically included and the Green's function is not needed, avoiding complicated computation.
3) *Generality*: The proposed DConvNet can be trained in free space, and directly used in a complex environment, instead of requiring retraining.
4) *Effectiveness*: The proposed approach only requires one-time far-field simulation or measurement.

II. Theory and Formulation

A. Problem Setup

A 2-D planar antenna array is considered in Fig. 1, where $N_x \times N_y$ units are equally spaced along the x-axis and y-axis, respectively. Each antenna unit is indexed by (N_x, N_y). The ideal far-field radiation pattern of this antenna array without considering antenna coupling in the direction (θ, φ) [21] is described as

$$E(\theta,\phi) = \sum_{n=0}^{N_y-1}\sum_{m=0}^{N_x-1} \omega_{n,m} * \exp\left(jm\frac{2\pi d_x}{\lambda} sin\theta cos\phi\right) \times \exp\left(jn\frac{2\pi d_y}{\lambda} sin\theta sin\phi\right) \quad (1)$$

where d_x and d_y are the antenna spacing, respectively, along the x-axis and y-axis, λ is the wavelength, and $\omega_{n,m}$ is the (n, m)th complex antenna weight. Notably, the proposed approach can also be applied to arbitrary antenna types and configurations.

Fig. 2 shows the simulated 3-D radiation patterns of a 3 × 3 planar patch array, as demonstrated in Fig. 1, where $N_x = 3$, $N_y = 3$, $d_x = 9$ mm, $d_y = 18.6$ mm, $L = 58$ mm, and $W = 31.4$ mm. Antennas are optimized to operate at 2.4 GHz with a mutual coupling of around −15 dB between adjacent elements. The comparison of Fig. 2(a) and (b) demonstrates that the failure of the first unit (1,1) leads to the reduction of the realized gain and the deflection of the radiation pattern of the antenna array. Hence, the far-field radiation data can be used to realize fault diagnosis in array.

B. Proposed ConvNet Architecture

In our approach, the far-field radiation pattern is input into the DConvNet model to predict the unit fault of the antenna array. Considering the difficulties of collecting training data in a large-scale by real experimental measurements, the simulated data are utilized as training data for our DConvNet. As the representative DL model, DConvNets can harness spatially oriented imagery as their data foundation [29], [30]. DConvNets are adept at leveraging intricate patterns within microwave field data, to facilitate accurate forecasting and identification in novel application contexts [20], [32]. Furthermore, despite the huge noise in a complex environment, DConvNets can still succeed in realizing prediction and recognition in the far-field [20], [32]. Therefore, during the training, we utilize simulated original data of radiation patterns (far-field radiation gains) as input to the proposed DConvNet and use the index of faulted antenna unit(s) on the array as the output. Thanks to the strong power of ConvNet, this method makes use of radiation patterns with strong interference to predict the faulted antenna unit in the antenna array. Thus, the proposed DConvNet can realize the diagnosis with high accuracy and efficiency.

TABLE I
DConvNet Architecture

Type	Filter Number	Filter Size	Stride	Input Size	Output Size
Convolution	30	3×1	[2, 1]	180×3×1	90×3×30
ReLu				90×3×30	90×3×30
Convolution	60	3×1	[3, 1]	90×3×30	30×3×60
ReLu				30×3×60	30×3×60
Convolution	180	3×1	[3, 1]	30×3×60	10×3×180
ReLu				10×3×180	10×3×180
Fully-connected				10×3×180	5400×1
Softmax				5400×1	45
Loss function					

The internal structure of our proposed model can be specifically presented at Fig. 3. Its input is a $M \times 3$ matrix with radiation pattern information, named as "radiation data," in which the three-column values stand for the received far-field radiation patterns (realized gains) (G) in xy, xz, and yz planes. For a straightforward depiction of the issue, the xy plane is referred to as the horizontal plane (H-plane), the xz plane as the first vertical plane (V1-plane), and the yz plane as the second vertical plane (V2-plane). Across each plane, M receivers are evenly distributed over the radiative angles (θ or φ), ranging from [0°, 180°].

For our proposed DConvNet, the features from the input are extracted by DConvNet layer by layer, followed by the final fully connected layer to predict the faulted unit of the antenna array. The specific parameters can be seen in Table I. The 1-D kernel is chosen for convolution operation. It has been widely employed in text natural language processing and stock prediction [33], [34]. The loss function of DConvNet is the half-mean-squared error [31].

The proposed approach is implemented in MATLAB 2020a with DL Toolbox [35]. The adaptive moment estimation (Adam) optimizer is applied to optimize the loss function. The Adam optimizer typically traverses the loss landscape more effectively [36]. Additionally, the batch normalization technique integrated within our DConvNet acts as a regularizing agent, enhancing the accuracy of predictions and mitigating the risk of overfitting [37], [38], [39].

The whole process could be summarized as the transformation process where the received far-field radiation pattern is transformed into the prediction of the faulted unit of the antenna array. In this process, the DConvNet directly takes "radiation data" G as its input, with the output being the index of the faulted antenna unit(s). Therefore, this DConvNet completely replaces traditional, computationally intensive methods, streamlining the entire operation [8], [9], [10], [11]. It is important that this DConvNet is entirely independent of calculating Green's function. Furthermore, the flexibility of this DL model is enhanced due to its data-driven nature, allowing it to incorporate additional prior knowledge through the training phase [40], [41]. Additionally, it is worth mentioning that our DConvNet architecture is designed to diagnose antenna arrays with a singular, unified model,

Authorized licensed use limited to: Missouri University of Science and Technology. Downloaded on January 16,2025 at 18:20:40 UTC from IEEE Xplore. Restrictions apply.

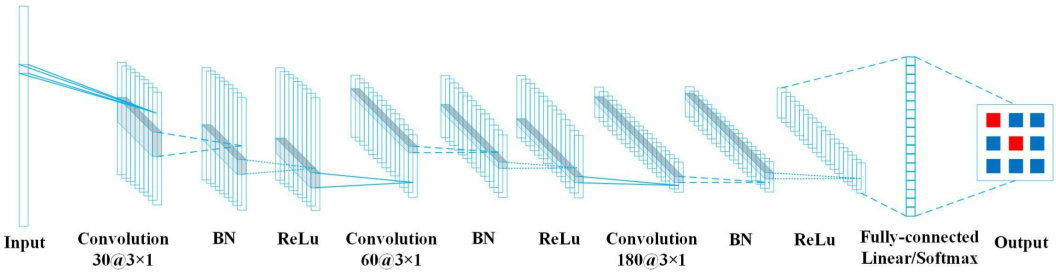

Fig. 3. DConvNet architecture for antenna array diagnosis with the repeated application of convolution, BN and ReLu layer.

offering a more streamlined solution compared to the multistep DL strategies for EM-based problems [42]. Plus, different from [39], [42], [43], this DConvNet realizes the transformation from far-field radiation into the prediction of faulted antenna unit and never requires the complicated computation for information compression or optimization in conventional diagnosis techniques.

Some issues need to be highlighted about the proposed model.

1) *Filtering in multichannel*: Filters exerted on the multichannel act as an important approach for ConvNet to amplify the power of the structure [38], [39], [42], [43], based on which several feature maps at each layer are created. Multichannel filtering in the proposed DConvNet can be referred to as a more efficient operation than conventional methods [38], [39], [42], [43].
2) *Computational complexity*: The primary operations governing the computational effort in our model are the repeated executions of convolution, BN, and ReLU. The computational demand is principally influenced by the convolutions employing compact filters [39], [43], [44]. Within the computation framework, the model processes inputs of size $N \times 3 \times 1$, utilizes R filters each of size $K \times 1$ for every layer, and spans f layers in depth. Consequently, the overall computational complexity of DConvNet is estimated to be in the order of $O(NKR^2f)$ [43], [44]. Additionally, the memory requirements for DConvNet are chiefly determined by the dimensions of the filters and biases, leading to a storage complexity estimated as $O(KR^2f)$ [43], [44].

C. Applying ConvNet to Antenna Array Diagnosis

By setting the receivers in the far-field around the tested antenna array, the radiation pattern of the antenna array can be noted for its nondamaged and various cases with the faulted unit(s). Then, the radiation data containing information of faulted antenna unit with high interference could get handled by our DConvNet, i.e., realizing the antenna array fault diagnosis. The designed procedures of the proposed approach for antenna array diagnosis are specifically described as three stages.

Step 1: *Collecting far-field radiation data*: The antenna array works in various faulted cases. In this process, the radiation gain G from the antenna array with faulted unit(s) is noted by far-field receivers.

Step 2: *DConvNet model training and testing*: To considerably enhance the noise tolerance and fault prediction accuracy of our proposed DL approach, the received radiation contaminated with noise has been utilized as input for our DConvNet for training and testing, which imitates the complicated environment in reality, including fabrication tolerance and the measurement tolerance. [45], [46]. Besides, as a typical numerical validation operation, the proposed DL approach is verified with 5% training data during the training, and the same validation operation is also done in the Section III-A–III-C. Meanwhile, the training output is the index of the corresponding faulted unit(s) on the antenna array. While we repeat the training and testing for several times to avoid the uncertainty of the proposed approach, Dropout operation during the testing is exerted during the testing step to make the model trustful [61], [62].

Step 3: *Far-field antenna array diagnosis*: Based on this trained DConvNet, the faulted unit on the antenna array can be recognized by using new received radiation even under huge interference.

III. Numerical Examples

A. Diagnosis for Antenna Array Using Three-Plane Radiation Gain

In Section III, a 3×3 planar antenna array is used, as demonstrated in Fig. 1, where $N_x = 3$, $N_y = 3$, $d_x = 9$ mm, $d_y = 18.6$ mm, $L = 58$ mm, and $W = 31.4$ mm. Following the designed diagnosis methodology in Section II, the specific process is as follows.

Step 1: Collecting far-field radiation data: The unit of the antenna array is faulted in various cases and the corresponding far-field realized radiation gains (G) at H, V1, and V2 planes are acquired by utilizing CST Microwave Studio [47]. In real cases, the far-field radiation gains (G) could be collected by receivers by using vector network analyzer (VNA).

Step 2: DConvNet model training and testing: During its training process, the input can be presented as a "image" matrix with the size of $M \times 3$ ($M = 180$). They [Fig. 4(d)–(f)] are formed by adding Gaussian noise to the ideally received radiation pattern information [Fig. 4(a)–(c)]. Here, considering interference in real scenario, we set its noise level to signal-to-noise ratio (SRN) up to 5 dB, which is generally much larger and rougher than the experimental-based cases [45], [46]. In Fig. 4, only the data resulted from the array with first, second, and fifth unit faulted are illustrated. In Fig. 4, it is evident that the ideally received radiation patterns are much different from the final "radiation data." We should highlight that the conventional approaches hardly realize the fault diagnosis for antenna array [48], due to this extremely small SNR. 45 000 "radiation data" with Gaussian noise are utilized to be input to train and test the proposed DConvNet, while their corresponding faulted unit of antenna array are selected as the outputs.

Step 3:Far-field antenna array diagnosis: To verify the validity of our DConvNet, another 4500 groups of "radiation data" are selected as inputs with Gaussian noise (SNR = 5 dB), while their corresponding faulted unit of the antenna array are utilized as outputs. As a consequence, the prediction of the faulted unit of the antenna array could be done in spite of such huge interference.

Fig. 5 shows the performances of this proposed DConvNet, where our proposed DConvNet can realize the antenna array diagnosis under large interference, with even zero error. In addition, more application of our approach demonstrate that our DConvNet trained by datasets (in any noise levels as SNR = 5 dB or SNR > 5 dB) all realize the antenna array diagnosis, with the same accuracy (zero error).

B. Diagnosis for Antenna Array Using One-Plane Radiation Gain

To increase practicality of this DL approach, we make two improvements about input data are as follows.

1) Instead of three planes, the inputs of our DConvNet only makes use of the far-field radiation gains (G) in H-plane.
2) In *Step 3*, the radiation angles of the received far-field radiation gains (G) are selected as $\phi = 0°, 3°, \ldots, 180°$.

Authorized licensed use limited to: Missouri University of Science and Technology. Downloaded on January 16,2025 at 18:20:40 UTC from IEEE Xplore. Restrictions apply.

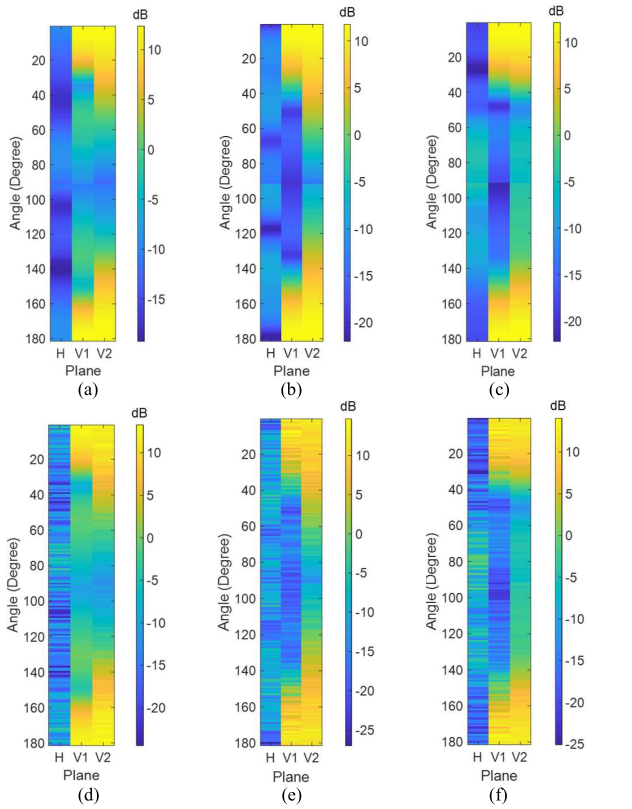

Fig. 4. Accurate "radiation data" for faulted unit (a) first unit, (b) second unit, and (c) fifth unit. "Radiation data" with noise for faulted unit (d) first unit, (e) second unit, and (f) fifth unit.

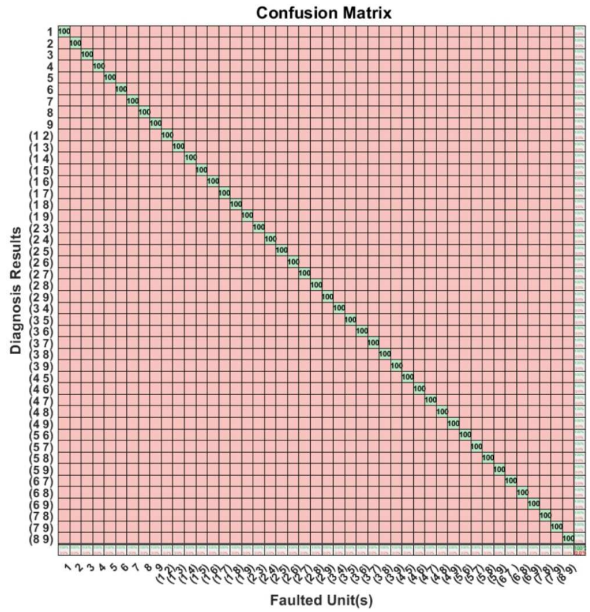

Fig. 5. Performance of the proposed approach for antenna array diagnosis. While the green percentage represents the success rate, the red percentage represents the failure rate for using three-plane far-field radiation gain and only using far-field radiation gains (G) in the H-plane.

As a consequence, the input of the DConvNet will be the $M/3$ vector, of which the size is smaller than the input matrix with the size of $M \times 3$, shown in the Section III-A. The detailed process can be described as follows.

Step 1: Collecting far-field radiation data: The unit of the antenna array is faulted in various cases and the corresponding far-field radiation gains (G) only in H-plane can be collected based on CST Microwave Studio.

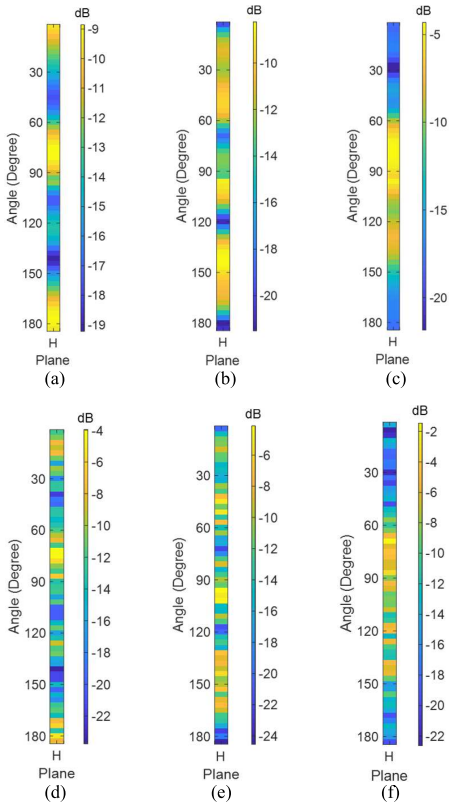

Fig. 6. Accurate "radiation data" in H-plane for faulted unit (a) first unit, (b) second unit, and (c) fifth unit. "Radiation data" in H-plane with noise for faulted unit (d) first unit, (e) second unit, and (f) fifth unit.

Step 2: DConvNet model training and testing: During its training process, the input is a "image" matrix with the size of $M \times 1$ ($M = 180$). Because the application scenario remains the same, Table I with the specific ConvNet parameters (stride size and kernel number) can still be made use of in this step. We set SRN up to 15 dB to form training data for the input, which is generally rougher than most of reported works [45], [46], shown in Fig. 6(a)–(c). 45 000 "radiation data" with Gaussian noise are utilized as the inputs to train and test the proposed DConvNet, while their corresponding faulted unit of the antenna array are selected to be the outputs.

Step 3:Far-field antenna array diagnosis: To verify the validity of our DConvNet, another 4500 groups of "radiation data" are selected as inputs with Gaussian noise (SNR = 10 dB), while the corresponding faulted unit of the antenna array are utilized as outputs. As described above, far-field radiation gain (G) is reduced to vector with the size of $M/3$. Thus, we utilize the linear interpolation method to make up for the received field data, based on which the input size can still be kept as $M \times 1$, presented in Fig. 6(d)–(f). Consequently, the prediction for the faulted units of the array can be done despite huge interference.

Fig. 5 shows the performances of this proposed DConvNet, where our proposed DConvNet can realize the antenna array diagnosis under huge interference.

C. Diagnosis for Antenna Array Using One-Plane Radiation Gain in Complex Environment

In Section C, this DL approach is applied to a more challenging scenario, shown in Fig. 7(a), where the arrangement positions the antenna array encircled by a concrete wall. The particular attributes of the concrete wall are characterized as follows: the material density is 2400 kg/m^3, the heat capacity is 0.8 kJ/K·kg, and the thermal conductivity is 1.7 W/K·m. The pattern of "radiation data" and the trained DConvNet in Section III-B is directly made use of here. The

Authorized licensed use limited to: Missouri University of Science and Technology. Downloaded on January 16,2025 at 18:20:40 UTC from IEEE Xplore. Restrictions apply.

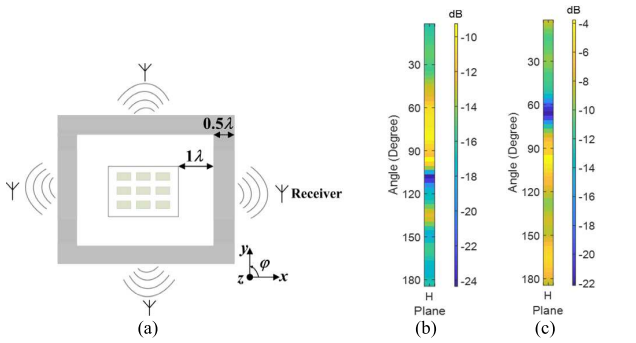

Fig. 7. (a) Top view of the faulted antenna array surrounded concrete walls. (b) Accurate "radiation data" in H-plane for the case with first unit faulted. (c) Interpolated "field data" in H-plane with noise for the case with first unit faulted.

TABLE II
DIAGNOSIS IN COMPLEX ENVIRONMENT

Faulted unit(s)	Success of diagnosis	Considering coupling effect	Computation of Green's function	Considering noise
1st unit	Yes	No	No	Yes
2nd and 5th units	Yes	No	No	Yes

precise "radiation data" in H-plane for unit fault diagnosis of the antenna array is presented in Fig. 7(b), while Fig. 7(c) illustrates the "field data" in H-plane with noise obtained from the interpolation method. Shown in Table II, we attempted two cases: 1) First unit on the antenna array is faulted; 2) both second and fifth are faulted on the antenna array. Compared with "field data" in H-plane in Section III-B, we can find the "field data" in this complex environment is much distinguished from the "field data" with Gaussian noise (i.e., seen as the totally new noise pattern). Furthermore, the proposed DConvNet can successfully recognize the faulted units on the antenna array, i.e., realize the antenna array diagnosis. We here need to emphasize that we train our DConvNet in free space but test it in a different complex environment to demonstrate its generality.

D. Discussion

From the numerical benchmarks above, we can see that the trainable DConvNet is capable of successfully recognizing the faulted units of antenna array even with large interference. Because of its strong feature-extracted capability for recognition [49], [51], the inevitable interference in reality will not affect the performance of recognition. Additionally, by using DConvNet, the environmental susceptibility and the complexity of Green's function computation for conventional methods can be avoided. Hence, this novel method demonstrates its possibility of being applied to the extremely harsh environment, including complex outer space with huge background radiation or highly packaged complex circuit. Plus, while the DConvNet is trained by data in free space, it can be directly used in a complex environment to diagnose antenna array, which demonstrates its generality. Three numerical examples above demonstrate the proposed approach can effectively realize antenna array diagnosis under big interference.

In addition, the proposed approach can successfully realize diagnosis for the array with the number of faulted unit larger than two. Following the designed diagnosis methodology in Section II, we have integrated together the cases with one, two, and three units faulted in training and testing. The proposed DL-based approach can still realize array diagnosis with 100% accuracy. While most of the diagnosis works focus on cases with total faulted units less than 20% [63], [64], our DL approach shows strong capability again.

Furthermore, though the training of our model is done on the small antenna arrays, the application of our approach can potentially be extended to the relative larger arrays, because the relative larger arrays can be discretized into several 3×3 antenna array (i.e., $N \times N$ arrays with $N > 3$ could be seen as the combination of a number of 3×3 arrays). During the diagnosis process, we can only exert operation on the individual 3×3 array and then move to another. For the relative larger arrays, we only need to simply do about $(N/3) \times (N/3)$, i.e., approximated to $(N \times N)/10$, times computation to accurately find the faulted unit on the relative larger arrays. In fact, our approach can make use of simple model and convenient measurement operation to realize antenna array diagnosis with high accuracy. The proposed method successfully avoids complicated theoretical computation and realizes antenna array diagnosis (even for large arrays) by simple measurement with high accuracy.

IV. CONCLUSION

In this communication, a DL approach for solving the problem of detecting unit failures in an array antenna is proposed. To realize the detection of unit failures in the phased array antenna, the received far-field radiation pattern is used to be the inputs of the proposed DConvNet, while the faulted unit(s) is utilized as its outputs. The probable strong interference in the real scenarios can be added to the training data. Various numerical benchmarks have illustrated the validity and generality of the proposed DConvNet for antenna array diagnosis. The computation of Green's function is never required in this DL approach. The proposed approach opens a new path for the real-time antenna array diagnosis in complex environments.

REFERENCES

[1] W. Chew et al., *Fast and Efficient Algorithms in Computational Electromagnetics*. Norwood, MA, USA: Artech House, 2001.
[2] M. Li and A. Abubakar, "Electromagnetic inverse problems [guest editorial]," *IEEE Antennas Propag. Mag.*, vol. 59, no. 5, pp. 9–115, Oct. 2017.
[3] F. Yang, R. Deng, S. Xu, and M. Li, "Design and experiment of a near-zero-thickness high-gain transmit-reflect-array antenna using anisotropic metasurface," *IEEE Trans. Antennas Propag.*, vol. 66, no. 6, pp. 2853–2861, Jun. 2018.
[4] R. C. Hansen, *Phased Array Antennas*, vol. 213. Hoboken, NJ, USA: Wiley, 2009.
[5] D. Jackson, "Phased array antenna handbook [book review]," *IEEE Antennas Propag. Mag.*, vol. 60, no. 6, pp. 124–128, Jul. 2018.
[6] B. Choudhury and R. M. Jha, *Soft Computing in Electromagnetics: Methods and Applications*. Cambridge, U.K.: Cambridge Univ. Press, 2016.
[7] C. A. Balanis, *Antenna Theory: Analysis and Design*. Hoboken, NJ, USA: Wiley, 2016.
[8] B.-K. Yeo and Y. Lu, "Array failure correction with a genetic algorithm," *IEEE Trans. Antennas Propag.*, vol. 47, no. 5, pp. 823–828, May 1999.
[9] J. A. Rodriguez-Gonzalez, F. Ares-Pena, M. Fernandez-Delgado, R. Iglesias, and S. Barro, "Rapid method for finding faulty elements in antenna arrays using far field pattern samples," *IEEE Trans. Antennas Propag.*, vol. 57, no. 6, pp. 1679–1683, Jun. 2009.
[10] M. D. Migliore, "A compressed sensing approach for array diagnosis from a small set of near-field measurements," *IEEE Trans. Antennas Propag.*, vol. 59, no. 6, pp. 2127–2133, Jun. 2011.
[11] B. Friedlander and T. Strohmer, "Bilinear compressed sensing for array self-calibration," in *Proc. 48th Asilomar Conf. Signals, Syst. Comput.*, Pacific Grove, CA, USA, Nov. 2014, pp. 363–367.
[12] C. M. Bishop, *Pattern Recognition and Machine Learning*. Berlin, Germany: Springer-Verlag, 2006.
[13] E. Alpaydin, *Introduction to Machine Learning*. Cambridge, MA, USA: MIT Press, 2020.
[14] Y. LeCun, Y. Bengio, and G. Hinton, "Deep learning," *Nature*, vol. 521, no. 7553, pp. 436–444, 2015.
[15] H. M. Yao, L. J. Jiang, and Y. W. Qin, "Machine learning based method of moments (ML-MoM)," in *Proc. IEEE Int. Symp. Antennas Propag. USNC/URSI Nat. Radio Sci. Meeting*, Jul. 2017, pp. 973–974.
[16] M. Li, T. Shan, F. Yang, and S. Xu, "Some investigations on applying deep learning techniques to solve partial differential equations," in *Proc. Int. Conf. Electromagn. Adv. Appl. (ICEAA)*, Granada, Spain, Sep. 2019, p. 879.
[17] T. Shan et al., "Study on a Poisson's equation solver based on deep learning technique," 2017, *arXiv:1712.05559*.

Authorized licensed use limited to: Missouri University of Science and Technology. Downloaded on January 16,2025 at 18:20:40 UTC from IEEE Xplore. Restrictions apply.

[18] H. M. Yao, L. Jiang, and M. Ng, "Implementing the fast full-wave electromagnetic forward solver using the deep convolutional encoder–decoder architecture," *IEEE Trans. Antennas Propag.*, vol. 71, no. 1, pp. 1152–1157, Jan. 2023.

[19] Z. Lin, K. Ji, M. Kang, X. Leng, and H. Zou, "Deep convolutional highway unit network for SAR target classification with limited labeled training data," *IEEE Geosci. Remote Sens. Lett.*, vol. 14, no. 7, pp. 1091–1095, Jul. 2017.

[20] S. Chen, H. Wang, F. Xu, and Y.-Q. Jin, "Target classification using the deep convolutional networks for SAR images," *IEEE Trans. Geosci. Remote Sens.*, vol. 54, no. 8, pp. 4806–4817, Aug. 2016.

[21] H. H. Zhang, L. J. Jiang, and H. M. Yao, "Embedding the behavior macromodel into TDIE for transient field-circuit simulations," *IEEE Trans. Antennas Propag.*, vol. 64, no. 7, pp. 3233–3238, Jul. 2016.

[22] H. H. Zhang, L. J. Jiang, H. M. Yao, and Y. Zhang, "Transient heterogeneous electromagnetic simulation with DGTD and behavioral macromodel," *IEEE Trans. Electromagn. Compat.*, vol. 59, no. 4, pp. 1152–1160, Aug. 2017.

[23] H. M. Yao and L. J. Jiang, "Machine learning based neural network solving methods for the FDTD method," in *Proc. IEEE Int. Symp. Antennas Propag. USNC/URSI Nat. Radio Sci. Meeting*, Boston, MA, USA, Jul. 2018, pp. 2321–2322.

[24] H. M. Yao and L. Jiang, "Machine-learning-based PML for the FDTD method," *IEEE Antennas Wireless Propag. Lett.*, vol. 18, no. 1, pp. 192–196, Jan. 2019.

[25] H. M. Yao and L. Jiang, "Enhanced PML based on the long short term memory network for the FDTD method," *IEEE Access*, vol. 8, pp. 21028–21035, 2020.

[26] T. Shan, M. Li, S. Xu, and F. Yang, "Synthesis of refiectarray based on deep learning technique," in *Proc. Cross Strait Quad-Regional Radio Sci. Wireless Technol. Conf. (CSQRWC)*, Jul. 2018, pp. 1–2.

[27] T. Shan, X. Pan, M. Li, S. Xu, and F. Yang, "Coding programmable metasurfaces based on deep learning techniques," *IEEE J. Emerg. Sel. Topics Circuits Syst.*, vol. 10, no. 1, pp. 114–125, Mar. 2020.

[28] A. Massa, D. Marcantonio, X. Chen, M. Li, and M. Salucci, "DNNs as applied to electromagnetics, antennas, and propagation—A review," *IEEE Antennas Wireless Propag. Lett.*, vol. 18, pp. 2225–2229, 2019.

[29] C. Dong, C. C. Loy, K. He, and X. Tang, "Image super-resolution using deep convolutional networks," *IEEE Trans. Pattern Anal. Mach. Intell.*, vol. 38, no. 2, pp. 295–307, Feb. 2016.

[30] B. Sahiner et al., "Classification of mass and normal breast tissue: A convolution neural network classifier with spatial domain and texture images," *IEEE Trans. Med. Imag.*, vol. 15, no. 5, pp. 598–610, Oct. 1996.

[31] H. M. Yao, W. E. I. Sha, and L. J. Jiang, "Applying convolutional neural networks for the source reconstruction," *Prog. Electromagn. Res. M*, vol. 76, pp. 91–99, 2018.

[32] H. M. Yao, M. Li, and L. Jiang, "Applying deep learning approach to the far-field subwavelength imaging based on near-field resonant metalens at microwave frequencies," *IEEE Access*, vol. 7, pp. 63801–63808, 2019.

[33] X. Ding, Y. Zhang, T. Liu and J. Duan, "Deep learning for event-driven stock prediction," in *Proc. 24th Int. Conf. Artif. Intell.*, 2015, pp. 2327–2333.

[34] K. Tymoshenko, D. Bonadiman, and A. Moschitti, "Convolutional neural networks vs. convolution kernels: Feature engineering for answer sentence reranking," in *Proc. Conf. North Amer. Chapter Assoc. Comput. Linguistics, Hum. Lang. Technol.*, 2016, pp. 1268–1278.

[35] P. Kim, *MATLAB Deep Learning*. New York, NY, USA: Apress, 2017.

[36] D. P. Kingma and J. L. Ba, "Adam: A method for stochastic optimization," in *Proc. Int. Conf. Learn. Represent.*, 2015, pp. 1–41.

[37] P. Luo, X. Wang, W. Shao, and Z. Peng, "Towards understanding regularization in batch normalization," in *Proc. ICLR*, 2019, pp. 1–23.

[38] H. M. Yao, L. Jiang, and W. E. I. Sha, "Enhanced deep learning approach based on the deep convolutional encoder–decoder architecture for electromagnetic inverse scattering problems," *IEEE Antennas Wireless Propag. Lett.*, vol. 19, pp. 1211–1215, 2020.

[39] L. Li, L. G. Wang, F. L. Teixeira, C. Liu, A. Nehorai, and T. J. Cui, "DeepNIS: Deep neural network for nonlinear electromagnetic inverse scattering," *IEEE Trans. Antennas Propag.*, vol. 67, no. 3, pp. 1819–1825, Mar. 2019.

[40] K. Belkebir, P. C. Chaumet, and A. Sentenac, "Superresolution in total internal reflection tomography," *J. Opt. Soc. Amer. A, Opt. Image Sci.*, vol. 22, no. 9, p. 1889, 2005.

[41] R. Guo, X. Song, M. Li, F. Yang, S. Xu, and A. Abubakar, "Supervised descent learning technique for 2-D microwave imaging," *IEEE Trans. Antennas Propag.*, vol. 67, no. 5, pp. 3550–3554, May 2019.

[42] H. M. Yao, W. E. I. Sha, and L. Jiang, "Two-step enhanced deep learning approach for electromagnetic inverse scattering problems," *IEEE Antennas Wireless Propag. Lett.*, vol. 18, no. 11, pp. 2254–2258, Nov. 2019.

[43] K. H. Jin, M. T. McCann, E. Froustey, and M. Unser, "Deep convolutional neural network for inverse problems in imaging," *IEEE Trans. Image Process.*, vol. 26, no. 9, pp. 4509–4522, Sep. 2017.

[44] J. Cong and B. Xiao, "Minimizing computation in convolutional neural networks," in *Proc. Int. Conf. Artif. Neural Netw.*, 2014, pp. 281–290.

[45] J. A. Russer and P. Russer, "Modeling of noisy EM field propagation using correlation information," *IEEE Trans. Microw. Theory Techn.*, vol. 63, no. 1, pp. 76–89, Jan. 2015.

[46] K. Haneda, E. Kahra, S. Wyne, C. Icheln, and P. Vainikainen, "Measurement of loop-back interference channels for outdoor-to-indoor full-duplex radio relays," in *Proc. 4th Eur. Conf. Antennas Propag.*, Apr. 2010, pp. 1–5.

[47] *3D EM Simulation Software*, Studio, CST Microw., Comput. Simul. Technol., Framingham, MA, USA, 2014.

[48] A. Neice, "Methods and limitations of subwavelength imaging," *Adv. Imag. Electron Phys.*, vol. 163, p. 117, Jan. 2010.

[49] A. Romero, C. Gatta, and G. Camps-Valls, "Unsupervised deep feature extraction for remote sensing image classification," *IEEE Trans. Geosci. Remote Sens.*, vol. 54, no. 3, pp. 1349–1362, Mar. 2016.

[50] Y. Chen, H. Jiang, C. Li, X. Jia, and P. Ghamisi, "Deep feature extraction and classification of hyperspectral images based on convolutional neural networks," *IEEE Trans. Geosci. Remote Sens.*, vol. 54, no. 10, pp. 6232–6251, Oct. 2016.

[51] V. Jain and S. Seung, "Natural image denoising with convolutional networks," in *Proc. Int. Conf. Neural Inf. Process. Syst.*, 2008, pp. 1–8.

[52] G. Chen, P. Shah, J. Stang, and M. Moghaddam, "Learning-assisted multimodality dielectric imaging," *IEEE Trans. Antennas Propag.*, vol. 68, no. 3, pp. 2356–2369, Mar. 2020.

[53] Z. Wei and X. Chen, "Deep-learning schemes for full-wave nonlinear inverse scattering problems," *IEEE Trans. Geosci. Remote Sens.*, vol. 57, no. 4, pp. 1849–1860, Apr. 2019.

[54] Z. Wei, D. Liu, and X. Chen, "Dominant-current deep learning scheme for electrical impedance tomography," *IEEE Trans. Biomed. Eng.*, vol. 66, no. 9, pp. 2546–2555, Sep. 2019.

[55] Y. Sanghvi, Y. Kalepu, and U. K. Khankhoje, "Embedding deep learning in inverse scattering problems," *IEEE Trans. Comput. Imag.*, vol. 6, pp. 46–56, 2020.

[56] D. Lin and Q. Wan, "Faulty elements diagnosis of phased array antennas using a generative adversarial learning-based stacked denoising sparse autoencoder," *J. Electromagn. Waves Appl.*, vol. 33, no. 3, pp. 382–407, Feb. 2019.

[57] T. Reimer, J. Sacristan, and S. Pistorius, "Improving the diagnostic capability of microwave radar imaging systems using machine learning," in *Proc. 13th Eur. Conf. Antennas Propag. (EuCAP)*, Mar. 2019, pp. 1–5.

[58] Y. H. Chang, J. L. Chen, and S. L. He, "Intelligent fault diagnosis of satellite communication antenna via a novel meta-learning network combining with attention mechanism," *J. Phys., Conf. Ser.*, vol. 1510, no. 1, Mar. 2020, Art. no. 012026.

[59] X. Wang, K. Konno, and Q. Chen, "Diagnosis of array antennas based on phaseless near-field data using artificial neural network," *IEEE Trans. Antennas Propag.*, vol. 69, no. 7, pp. 3840–3848, Jul. 2021.

[60] K. Chen, W. Wang, X. Chen, and H. Yin, "Deep learning based antenna array fault detection," in *Proc. IEEE 89th Veh. Technol. Conf.*, Apr. 2019, pp. 1–5.

[61] Z. Wei and X. Chen, "Uncertainty quantification in inverse scattering problems with Bayesian convolutional neural networks," *IEEE Trans. Antennas Propag.*, vol. 69, no. 6, pp. 3409–3418, Jun. 2021.

[62] Y. Gal and Z. Ghahramani, "Dropout as a Bayesian approximation: Representing model uncertainty in deep learning," in *Proc. Int. Conf. Mach. Learn.*, 2016, pp. 1050–1059.

[63] S. U. Khan, M. K. A. Rahim, M. Aminu-Baba, A. E. K. Khalil, and S. Ali, "Diagnosis of faulty elements in array antenna using nature inspired cuckoo search algorithm," *Int. J. Electr. Comput. Eng. (IJECE)*, vol. 8, no. 3, p. 1870, Jun. 2018.

[64] B. Fuchs, L. L. Coq, and M. D. Migliore, "Fast antenna array diagnosis from a small number of far-field measurements," *IEEE Trans. Antennas Propag.*, vol. 64, no. 6, pp. 2227–2235, Jun. 2016, doi: 10.1109/TAP.2016.2547023.

Authorized licensed use limited to: Missouri University of Science and Technology. Downloaded on January 16,2025 at 18:20:40 UTC from IEEE Xplore. Restrictions apply.